

NON-LINEAR RESPONSE OF TORSIONALLY COUPLED BASE ISOLATED STRUCTURE TO HARMONIC EXCITATION

R.S.JANGID* and T.K.DATTA**

Effect of base isolation on the response of torsionally coupled system under harmonic base excitation is investigated with the help of a 3-D idealized model of building. The base isolator of the building allows translational as well as rotational displacements at the base level of the building model. The hysteretic force deformation characteristics of the bearing are modeled by coupled non-linear differential equations. The responses of the base isolated system are compared with that of the fixed base system in order to study the effectiveness of base isolation. The investigation shows (i) the response of base isolated system for different frequencies of base excitation with respect to fixed base frequencies of the system, (ii) the difference in the response obtained by considering and ignoring the interaction between the restoring forces of the elastomeric bearings and (iii) the effect of torsional coupling on the effectiveness of base isolation.

Key Words : base isolation, torsionally coupled system, base excitation

INTRODUCTION

The use of base isolators for aseismic design of structures has attracted considerable attention in recent years. The main concept is to isolate the structure from ground instead of the conventional techniques of strengthening the structural member. This new design methodology appears to have considerable potential in preventing earthquake damage of structure and their internal equipment. The devices which isolate the structure at its base have two important characteristics : horizontal flexibility and energy absorbing capacity. Flexibility as such reduces the natural frequency of the structure lower than the energy containing frequencies of earthquake excitation. Energy absorbing capacity reduces both base displacement and seismic energy being transmitted to the building. In designing a base isolated structure the aims are : (1) to provide a relatively stiff superstructure that will behave like a rigid body with little interstorey drift and (2) to concentrate most of the horizontal deformation to the flexible mounting that supports the structure. One of the most attractive devices is the laminated rubber bearing which offers various advantages, such as lower cost than other devices, simplification of layout and high damping at small level of amplitude. Among the different types of bearings, the laminated rubber bearing (LRB system) or the lead rubber bearing system has been used widely in New Zealand. The effectiveness of base isolation has been demonstrated both experimentally^(6),8),13) and analytically^(1)-4),7),12). In the past twenty years, many practical base isolation

devices have been provided in many buildings. An excellent review on base isolation is presented by Kelly⁽⁵⁾.

The analytical works on base isolation of buildings deal with 2-D idealization which is strictly valid for symmetric buildings or, buildings with very small eccentricity or, buildings torsionally very stiff. Very few analytical works are reported on the seismic base isolation of 3-D building models. Pan and Kelly⁽¹¹⁾ studied the effect of eccentricity on the elastic response of torsionally coupled base isolated system. Recently, Nagara-jaiha and et al.⁽⁹⁾ studied the nonlinear response of 3-D base isolated building to EL Centro earthquake motion. Clearly, there is a lack of studies on the subject especially in exploring the parametric behaviour of torsionally coupled base isolated system.

Here-in, the parametric behaviour of a 3-D torsionally coupled hysteretic base isolated system is investigated under harmonic ground motion. In specific terms, the objectives of the study are : (i) to show how the variation of response of such base isolated system is influenced by the ratio of excitation frequency to system frequency (fixed base), (ii) to distinguish between the response characteristics of torsionally coupled and uncoupled base isolated systems, (iii) to investigate the behaviour of base isolated system under different important parametric variations and (iv) to illustrate how the bidirectional interaction of restoring forces in the bearing effect the response of base isolated building model as compared to the response without interaction (uniaxial model of bearing).

* Research Scholar

** Professor, Department of Civil Engineering Indian Institute of Technology, New Delhi-110016

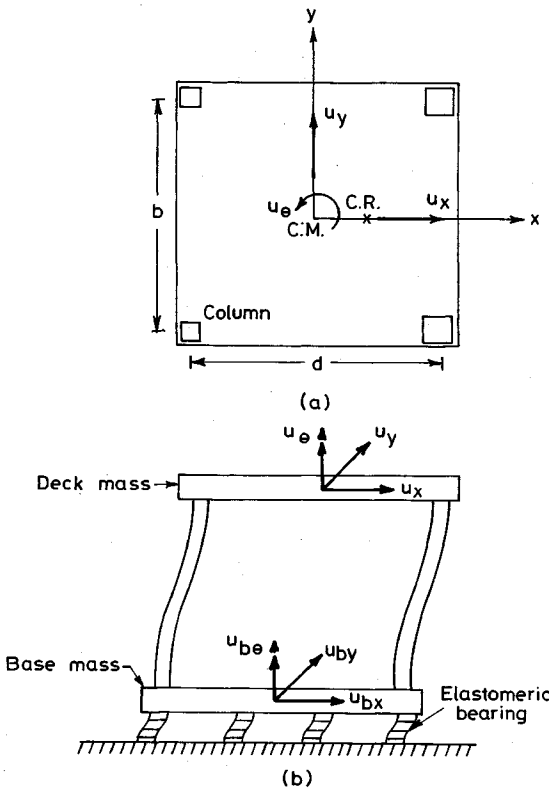


Fig.1 Structural model

STRUCTURAL AND BASE ISOLATION MODEL

Fig.1 shows the structural system considered, which is an idealized one storey building model mounted on isolator. The rigid deck mass is supported by columns. Each column has the same stiffness in the two principle directions. The torsional mass of the deck is varied to provide various uncoupled torsional to lateral frequency ratio (for fixed base). This is accomplished by introducing additional lumped masses symmetrically arranged about the centre of mass of the rigid deck. By manipulating the distance of the lumped masses from the centre of mass, the torsional mass of the deck is varied without disturbing the position of the centre of mass. Note that the size and mass of the rigid deck and the base slab, as well as the total lumped masses corresponding to the translational degrees of freedom remain unaltered. Consequently, the layout of the isolators remains unaffected when the torsional mass is varied to change the uncoupled torsional frequency of the fixed base system. The force deformation characteristics of the columns is assumed to be elastic.

The base isolator consists of an array of elastomeric bearings arranged between the base

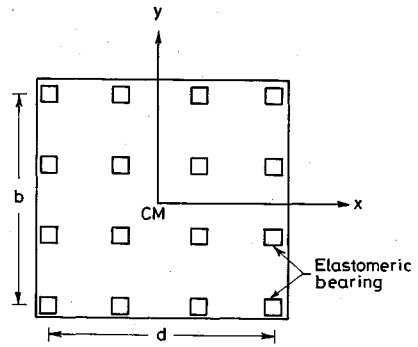


Fig.2 Arrangement of the bearings

mass and the foundation as shown in Fig.2. The stiffness distribution of the columns is symmetric about the *x*-axis but not about the *y*-axis, as a result the system will display torsional effect when excited in the lateral direction *-y*. Two lateral, *u_x* and *u_y* and one rotational, *u_θ* degrees of freedom are considered at the center of the deck mass (relative to the base mass). The isolator permits the base motions relative to the ground in two lateral directions i.e. in directions *u_{bx}* and *u_{by}* and a rotation *u_{bθ}* about the vertical axis as shown in Fig.1.b. Further, the isolator is assumed to carry the vertical load without undergoing any vertical deformation. A corresponding fixed base system or unisolated system is the same system without elastomeric bearing and base mass restrained against all movements.

Let *k_{ix}* and *k_{iy}* represent the lateral stiffness of the *ith* column in *x*- and *y*-directions. Then

$$K_x = \sum_i k_{ix} \text{ and } K_y = \sum_i k_{iy} \dots \dots \dots (1)$$

are the lateral stiffness of the fixed base system in the *x*- and *y*-directions, respectively. Let *x_i* and *y_i* denote the *x*- and *y*- coordinates of *ith* column with respect to the center of the mass, respectively. Then, the total torsional stiffness of the system defined at the center of the mass is given by

$$K_\theta = \sum_i (k_{ix}y_i^2 + k_{iy}x_i^2) \dots \dots \dots (2)$$

in which the torsional stiffness of each individual column element is negligible and is not included. The three uncoupled frequency parameters *w_x*, *w_y* and *w_θ* are defined as follow :

$$w_x = \sqrt{\frac{K_x}{m}} ; w_y = \sqrt{\frac{K_y}{m}} \text{ and } w_\theta = \sqrt{\frac{K_\theta}{mr^2}} \dots \dots (3)$$

in which *m* is the mass of rigid deck including additional lumped masses : *r* is the radius of gyration about vertical axis at the center of the mass ; These frequencies may be interpreted as the natural frequencies of the fixed base system if it were torsionally uncoupled i.e. a system with *e_x*=

0, but, m , K_x and K_y the same as in the coupled system. $T_x=2\pi/w_x$ is the corresponding uncoupled time period.

The eccentricity between the center of the mass (CM) and the center of resistance (CR) is given by

$$e_x = \frac{1}{K_y} \sum_i k_{iy} x_i \dots\dots\dots (4)$$

The force deformation relationship of elastomeric bearing in translational directions is mathematically idealized by the empirical equations suggested by Park and et al¹⁰. The restoring forces, F_{xi} and F_{yi} of the i^{th} elastomeric bearing (isotropic) in x - and y -directions are given by the relation :

$$\begin{Bmatrix} F_{xi} \\ F_{yi} \end{Bmatrix} = \alpha k_0 \begin{Bmatrix} U_{xi} \\ U_{yi} \end{Bmatrix} + (1-\alpha) k_0 \begin{Bmatrix} Z_{xi} \\ Z_{yi} \end{Bmatrix}$$

or, $\{F_i\} = \alpha k_0 \{U_i\} + (1-\alpha) k_0 \{Z_i\} \dots\dots\dots (5)$

in which U_{xi} and U_{yi} are the displacements, and Z_{xi} and Z_{yi} are a function of U_{xi} and U_{yi} and provide hysteretic component of restoring force when multiplied by $(1-\alpha)k_0$ in x - and y -directions, respectively ; α is the post to pre-yielding stiffness ratio ; $k_0=Q/q$ is the initial stiffness ; Q and q are the yield force and displacement to the bearings respectively ; Z_{xi} and Z_{yi} satisfy the following coupled non-linear first order differential equations :

$$\begin{aligned} \{\dot{Z}_i\} &= [G] \{\dot{U}_i\} \dots\dots\dots (6) \\ [G] &= \end{aligned}$$

$$\begin{bmatrix} A - \beta \text{sgn}(\dot{U}_{xi}) |Z_{xi}| Z_{xi} - \tau Z_{xi}^2 & -\beta \text{sgn}(\dot{U}_{yi}) |Z_{yi}| Z_{xi} - \tau Z_{xi} Z_{yi} \\ -\beta \text{sgn}(\dot{U}_{xi}) |Z_{xi}| Z_{yi} - \tau Z_{xi} Z_{yi} & A - \beta \text{sgn}(\dot{U}_{yi}) |Z_{yi}| Z_{yi} - \tau Z_{yi}^2 \end{bmatrix}$$

..... (7)

in which β , τ and A are the parameters which control the shape and size of hysteresis loop. sgn denotes the signum function. The force displacement behaviour of elastomeric bearing can be modeled by selecting properly the parameters Q , q , α , β , τ and A . An additional viscous damping is assumed to be provided by the individual bearing in the lateral directions.

Two typical smooth hysteresis loops of bearing using Equations (5)~(7) under sinusoidal displacement of amplitude 0.1 m and frequency of 1 Hz. in x - and y -directions are shown in Fig.3. The parameters are : $Q=250$ ton, $q=0.025$ m, $\alpha=0$ (elasto-plastic), $\beta=\tau=0.5/q^2$ and $A=1$. The loop for no interaction case represents the independent uniaxial model of bearing in two orthogonal directions reported in Reference 14). This is obtained by neglecting the effect of force interaction i.e. by replacing the off-diagonal element of the matrix, $[G]$ in Equation (7), by zero. The difference between the two hysteresis loops is that

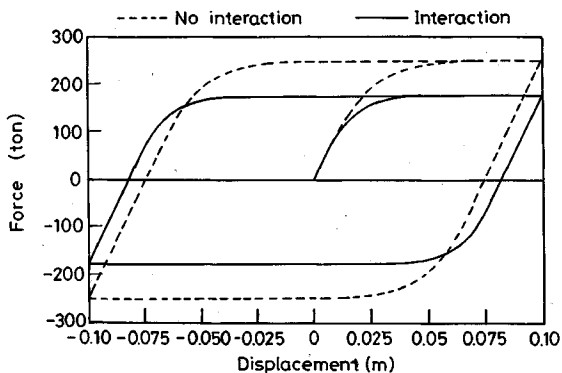


Fig.3 Force deformation characteristic of the bearing.

when the force interaction is taken into account the bearing starts yielding at the lower value of yield strength.

Equations of Motion

The equations of motion of the system under consideration are written as :

$$[M] \{\ddot{u} + \ddot{u}_b\} + [C] \{\dot{u}\} + [K] \{u\} = -[M][r] \{\ddot{u}_g\} \dots\dots\dots (8)$$

$$[M_b] \{\ddot{u}_b\} + [C_b] \{\dot{u}_b\} + \{F_b\} - [C] \{\dot{u}\} - [K] \{u\} = -[M_b][r] \{\ddot{u}_g\} \dots\dots\dots (9)$$

in which $[M]$, $[K]$ and $[C]$ are the lumped mass, stiffness and damping matrices corresponding to the DOF at the deck ; $\{u\} = [u_x, u_y, u_\theta]^T$, vector of displacements at the deck relative to the base mass ; $[M_b]$ and $[C_b]$ are the lumped mass and damping matrices corresponding to the DOF at the base mass ; $\{F_b\}$ is the total force vector of restoring force mobilized in the elastomeric bearing ; $\{u_b\} = [u_{bx}, u_{by}, u_{b\theta}]^T$; $\{\ddot{u}_g\} = [\ddot{u}_{gx}, \ddot{u}_{gy}]^T$, \ddot{u}_{gx} and \ddot{u}_{gy} are the random ground accelerations in x - and y -directions respectively ; and $[r]$ is the matrix of earthquake influence coefficient. The stiffness matrices, $[K]$, restoring force vector, $\{F_b\}$ and damping matrix, $[C_b]$ are written as :

$$[K] = \sum_i [T_i]^T [k_i] [T_i] \dots\dots\dots (10)$$

$$[k_i] = \text{diag} [k_{ix}, k_{iy}] \dots\dots\dots (11)$$

$$[T_i] = \begin{bmatrix} 1 & 0 & -y_i \\ 0 & 1 & x_i \end{bmatrix} \dots\dots\dots (12)$$

$$\{F_b\} = \sum_i [T_{ib}]^T \{F_i\} \dots\dots\dots (13)$$

$$[C_b] = \sum_i [T_{ib}]^T [c_{ib}] [T_{ib}] \dots\dots\dots (14)$$

$$[T_{ib}] = \begin{bmatrix} 1 & 0 & -y_{ib} \\ 0 & 1 & x_{ib} \end{bmatrix} \dots\dots\dots (15)$$

$$[c_{ib}] = \text{diag} [c_{ixb}, c_{iyb}] \dots\dots\dots (16)$$

in which $[T_i]$ and $[T_{ib}]$ are the transformation matrices for column and bearing, respectively; and x_{bi} and y_{bi} denote the x - and y -coordinates of the i^{th} bearing with respect to the center of base mass, respectively. F_{xi} and F_{yi} are the restoring force of the i^{th} bearing in x - and y -directions, respectively which are obtained from Equations (5) ~ (7). Although, a torsional moment develops at each bearing, but the contribution of this torsional moment to the total torque exerted at the base mass is insignificant and hence, it is not included. The moments of F_{xi} and F_{yi} about the center of the base mass are assumed to provide the base torsional restraint. c_{ixb} and c_{iyb} are the viscous damping of the i^{th} bearing in x - and y -directions, respectively. c_{ixb} and c_{iyb} are given as^(1,2) :

$$c_{ixb} = 2\xi_{ixb}(k_0 m_{ib})^{1/2} \dots \dots \dots (17)$$

$$c_{iyb} = 2\xi_{iyb}(k_0 m_{ib})^{1/2} \dots \dots \dots (18)$$

ξ_{ixb} and ξ_{iyb} are the damping constants of the bearing in x - and y -directions, respectively; m_{ib} is the lumped base mass on the bearing.

Incremental solution procedure

Since the restoring forces of the elastomeric bearings are nonlinear functions of the displacement and velocity, the equations of motion are to be solved in the incremental form. Newmark's β method⁹ is chosen for the solution of differential equations of motion, assuming the linear variation of acceleration over small time interval, δt . In the incremental form, equations (Equations 8-9) can be written as :

$$[M] \{ \delta \ddot{u} + \delta \dot{u}_b \} + [C] \{ \delta \dot{u} \} + [K] \{ \delta u \} = - [M] [r] \{ \delta \ddot{u}_g \} \dots \dots (19)$$

$$[M_b] \{ \delta \ddot{u}_b \} + [C_b] \{ \delta \dot{u}_b \} + \{ \delta F_b \} - [C] \{ \delta \dot{u} \} - [K] \{ \delta u \} = - [M_b] [r] \{ \delta \ddot{u}_g \} \dots \dots (20)$$

Incremental force vector, $\{ \delta F_b \}$ from equation 13) can be written as :

$$\{ \delta F_b \} = \sum_i [T_{ib}]^T \{ \delta F_i \} \dots \dots \dots (21)$$

$$\{ \delta F_i \} = \alpha k_0 \{ \delta U_i \} + (1 - \alpha) k_0 \{ \delta Z_i \} \dots \dots (22)$$

$$\{ \delta U_i \} = [T_{ib}] \{ \delta u_b \} \dots \dots \dots (23)$$

Following the assumption of linear variation of acceleration over the time interval δt , the incremental vector $\{ \delta \ddot{u} \}$ and $\{ \delta \dot{u} \}$ are given as :

$$\{ \delta \ddot{u} \} = a_0 \{ \delta u \} + a_1 \{ \dot{u}^t \} + a_2 \{ \ddot{u}^t \} \dots \dots (24)$$

$$\{ \delta \dot{u} \} = b_0 \{ \delta u \} + b_1 \{ \dot{u}^t \} + b_2 \{ \ddot{u}^t \} \dots \dots (25)$$

in which $a_0 = 6/\delta t^2$; $a_1 = -6/\delta t$; $a_2 = -3$; $b_0 = 3/\delta t$; $b_1 = -3$; and $b_2 = -\delta t/2$. Superscript denotes the time. Similarly, $\{ \delta \ddot{u}_b \}$ and $\{ \delta \dot{u}_b \}$ can be obtained by replacing u by u_b in Equations (24) and (25). Equations (19) and (20) may be written as :

$$\begin{bmatrix} K_{uu} & K_{uub} \\ K_{ubu} & K_{ubub} \end{bmatrix} \begin{bmatrix} \delta u \\ \delta u_b \end{bmatrix} = \begin{bmatrix} \delta P_u \\ \delta P_{ub} \end{bmatrix} \dots \dots \dots (26)$$

$$K_{uu} = a_0 [M] + b_0 [C] + [K] \dots \dots \dots (27)$$

$$K_{uub} = a_0 [M] \dots \dots \dots (28)$$

$$K_{ubu} = -b_0 [C] - [K] \dots \dots \dots (29)$$

$$K_{ubub} = a_0 [M_b] + b_0 [C_b] + \alpha k_0 \sum_i [T_{ib}]^T [T_{ib}] \dots \dots \dots (30)$$

$$\delta P_u = - [M] [r] \{ \delta \ddot{u}_g \} - \{ a_1 [M] + b_1 [C] \} \{ \dot{u}^t \} - \{ a_2 [M] + b_2 [C] \} \{ \ddot{u}^t \} - \{ a_1 [M] \} \{ \dot{u}_b^t \} - \{ a_2 [M] \} \{ \ddot{u}_b^t \} \dots \dots \dots (31)$$

$$\delta P_{ub} = - [M_b] [r] \{ \delta \ddot{u}_g \} - (1 - \alpha) k_0 \sum_i [T_{ib}]^T \{ \delta Z_i \} - \{ a_1 [M_b] + b_1 [C_b] \} \{ \dot{u}_b^t \} - \{ a_2 [M_b] + b_2 [C_b] \} \{ \ddot{u}_b^t \} + \{ b_1 [C] \} \{ \dot{u}^t \} + \{ b_2 [C] \} \{ \ddot{u}^t \} \dots \dots \dots (32)$$

In order to solve incremental Equation (26), δP_u and δP_{ub} as given by equations (31) and (32) should be known at any time step. Since δP_{ub} involves incremental hysteretic displacement component, $\{ \delta Z_i \}$ for each bearing, which in turn depend on incremental based displacement $\{ \delta u_b \}$ at the current time step, an iterative procedure is required to obtain the incremental solution. In the iterative procedure, the value of $\{ \delta Z_i \}$ at each time step is obtained by solving Equation (6) with the help of Runge-Kutta method. The steps of the procedure are as follow :

1. Assume $\{ \delta Z_i \}_j = 0$ in iteration $j=1$
2. Substitute $\{ \delta Z_i \}_j$ in Equation (32) and solve Equation (26).
3. Calculate velocity vector $\{ \dot{u}_b^{t+\delta t} \}$
4. Compute the revised $\{ \delta Z_i \}_{j+1}$ for each bearing using the Runge-Kutta method which are given by :

$$\{ \delta Z_i \} = \frac{K_{0i} + 2K_{1i} + 2K_{2i} + K_{3i}}{6} \dots \dots \dots (33)$$

$$K_{0i} = \delta t G(Z_i) [T_{ib}]^T \{ \dot{u}_b^t \} \dots \dots \dots (34)$$

$$K_{1i} = \delta t G(Z_i + K_{0i}/2) [T_{ib}]^T \{ \dot{u}_b^{t+\delta t/2} \} \dots \dots (35)$$

$$K_{2i} = \delta t G(Z_i + K_{1i}/2) [T_{ib}]^T \{ \dot{u}_b^{t+\delta t/2} \} \dots \dots (36)$$

$$K_{3i} = \delta t G(Z_i + K_{2i}/3) [T_{ib}]^T \{ \dot{u}_b^{t+\delta t} \} \dots \dots (37)$$

The quantity inside the bracket (.) denotes the value of the vector $\{ Z_i \}$ to be taken in the matrix $[G]$ given by Equation (7).

5. Iterate further, until the following convergence criterion is satisfied for each bearing

$$\frac{|\{\delta Z_i\}_{j+1}| - |\{\delta Z_i\}_j|}{Z_m} \leq \text{Tolerance} \dots\dots\dots (38)$$

$$Z_m = \sqrt{\frac{A}{\beta + \tau}} \dots\dots\dots (39)$$

When the convergence criterion is satisfied, the incremental vectors $\{\delta u\}$, $\{\delta u_b\}$, $\{\delta \dot{u}\}$ and $\{\delta \dot{u}_b\}$ are obtained from Equations (25) and (26). With $\{\delta u_b\}$, $\{\delta \dot{u}_b\}$ and $\{\delta Z_i\}$ known, $\{\delta F_i\}$ and $\{\delta F_b\}$ are calculated using Equations (21) and (22), and added to the values of $\{F_i\}$ and $\{F_b\}$ at the previous time step to obtain these at the current time step. Finally, the acceleration vectors $\{\ddot{u}\}$ and $\{\ddot{u}_b\}$ for the current time step are evaluated directly from the equations (8) and (9), respectively.

PARAMETRIC STUDY

A large number of parameters influence the responses of the system. Effects of only a few important parameters are considered here which predominantly influence the torsional coupling and base isolation characteristics. They are : uncoupled time period (T_x), ratio of torsional to lateral frequency of fixed base (w_b/w_x), mass ratio (m_b/m), eccentricity ratio (e_x/d), level of the yield strength of bearing (Q), post to pre-yielding stiffness ratio (α) and ratio of excitation frequency to uncoupled fixed base frequency (Ω/w_x). The specifications for the values of the other parameters (held constant throughout) are : $m=40$ ton. sec^2/m ; $b=d=6$ m ; number of hysteretic dampers, $N=4$; modal damping for the super-structure= 5% for all modes ; viscous damping $\xi_{ixb} = \xi_{iyb} = 10\%$; $q=0.025$ meter ; $\beta=0.5/q^2$; $\tau=0.5/q^2$; and $A=1$. Note that the elastomeric bearings are symmetrically placed below the base mass.

In order to study the effectiveness of base isolation and the effect of torsional coupling, it is convenient to express the response in terms of the ratio rather than plotting their values. For this purpose, response ratio R is defined as :

$$R = \frac{\text{Maximum response of asymmetric base isolated system}}{\text{Maximum response of corresponding fixed base system}}$$

The response ratio R is an index of the performance of base isolation system and the value less than unity indicates that the base isolation is effective. The earthquake excitation is considered as a harmonic ground motion with amplitude of 0.25 g in x -and y -directions. Since the two components of ground motions are the same, the effect of torsional coupling on the response of asymmetric base isolated system is primarily exhibited in the response corresponding to the displacements u_y , u_{by} (which are perpendicular to the direction of eccentricity) and u_θ , $u_{b\theta}$. Note that for the case of symmetric base isolated system,

Table 1

Mode	1	2	3	4	5	6	
Natural Frequency of base isolated system (rad/sec)	3.63	3.75	4.32	8.02	8.38	12.72	
Corresponding fixed base frequencies	5.05	6.28	7.31	-	-	-	
Node-shapes	u_x	0.000	0.417	0.000	0.000	-1.891	0.000
	u_y	0.516	0.000	0.120	1.788	0.000	0.520
	u_θ	0.084	0.000	0.161	0.124	0.000	-0.547
	u_{bx}	0.000	0.753	0.000	0.000	0.827	0.000
	u_{by}	0.650	0.000	-0.378	-0.805	0.000	-0.193
	$u_{b\theta}$	0.040	0.000	0.159	-0.139	0.000	0.403

effectiveness of base isolation will be identical for displacements in x -and y -directions.

For the parametric study, sinusoidal ground acceleration in the two directions i.e. $\ddot{u}_{gx} = \ddot{u}_{gy} = 0.25 \text{ g sin}(\Omega t)$ and the values of excitation frequency, Ω are taken as $0.25 w_x$, w_x and $2 w_x$; in which w_x is the fixed base natural frequency defined in Equation (3). In addition, the effect of post to pre yielding ratio, α which defines the bi-linear stiffness characteristics of the bearings, is also investigated.

Since the base isolators undergo inelastic deformation during earthquake, the system does not have unique natural frequencies and mode-shapes. However, in order to get an estimate of the amount of flexibility introduced to the system by the isolators, the natural frequencies of the base isolated structure obtained by considering the initial stiffness (tangent stiffness) of the isolators are compared with those of the fixed base system in **Table 1**. In the same table, the mode-shapes coefficients of the base isolated system are also shown. It is observed from the table that the fundamental period of the isolated system is elongated by about 43% compared to the fixed base system. Further, all the modes of the system are found to be coupled.

Before conducting the parametric study, the influence of harmonic excitation frequency, Ω on the response of the base isolated system is studied.

Influence of Ω on the Effectiveness of Base Isolation

The variations of R for the response u_x with frequency ratio Ω/w_x for uncoupled time period, $T_x = 0.5, 1.0$ and 1.5 sec are shown in **Fig.4**. The nature of variation is similar for all values of uncoupled time period, T_x . However, the response ratio is higher for higher value of T_x . Thus, base isolation is more effective for relatively rigid structure. It is to be noted that base isolation is effective in the range of excitation frequency $\Omega/w_x > 0.5$ except for very flexible structure i.e. $T_x = 1.5$ sec. Further, the response ratio becomes

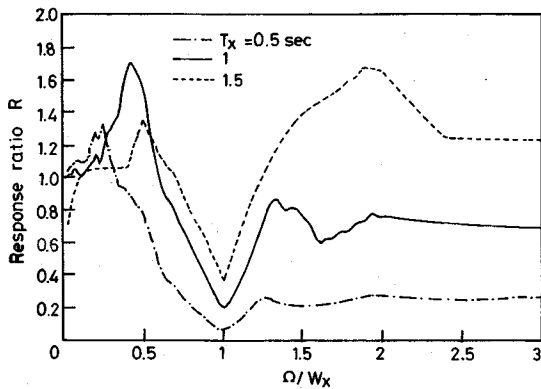


Fig.4 Variation of response ratio R for response u_x . $e_x/d=0.25$, $m_b/m=2$, $w_\theta/w_x=1$, $Q=50$ ton and $\alpha=0$.

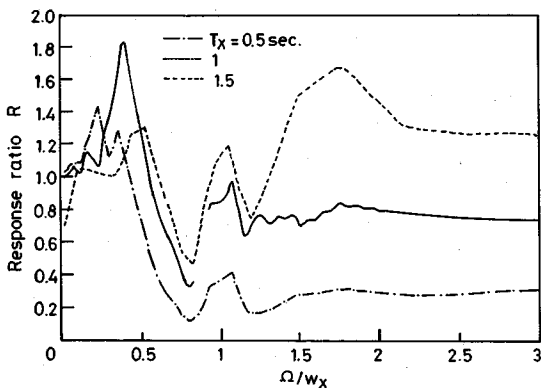


Fig.5 Variation of response ratio R for response u_y . $e_x/d=0.25$, $m_b/m=2$, $w_\theta/w_x=1$, $Q=50$ ton and $\alpha=0$.

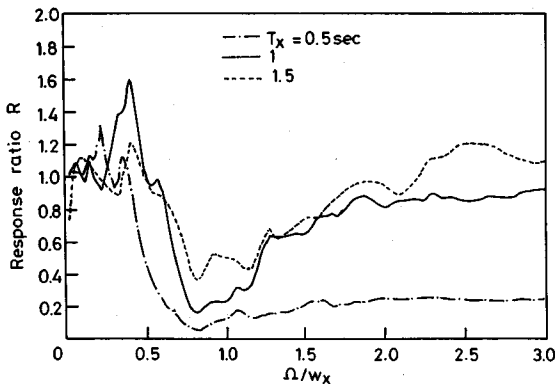
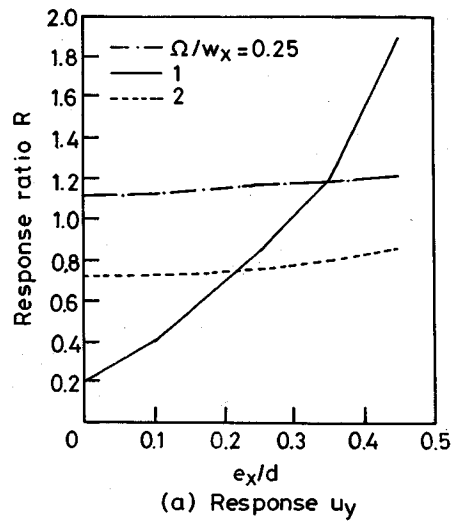
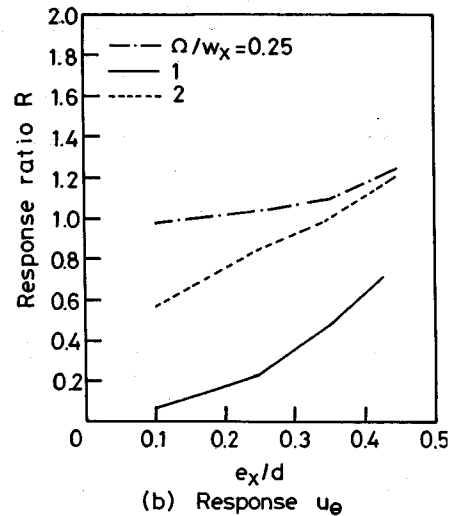


Fig.6 Variation of response ratio R for response u_θ . $e_x/d=0.25$, $m_b/m=2$, $w_\theta/w_x=1$, $Q=50$ ton and $\alpha=0$.

minimum when the frequency ratio is nearly unity. This is the case because at $\Omega/w_x=1$, the response of the fixed base system becomes maximum due to resonating effect and therefore, the value of the response ratio for response u_x becomes minimum. For very low frequency of excitation ($\Omega/w_x < 0.5$),



(a) Response u_y



(b) Response u_θ

Fig.7 Variation of ratio R for u_y and u_θ against e_x/d . $T_x=1$ sec., $m_b/n=2$, $w_\theta/w_x=1$, $Q=50$ ton and $\alpha=0$.

the base isolation becomes ineffective for the structure which is not very flexible (i.e. $T_x < 1.5$ sec).

The variations of R for u_y and u_θ against frequency ratio, Ω/w_x are shown in Fig.5 and 6, respectively. The variations are similar to that for response u_x as shown in Fig.4, except the difference that the response ratios become minimum not at exactly $\Omega/w_x=1$, but in the vicinity of it. This happens due to the effect of torsional coupling.

Effect of Eccentricity

The variations of R for responses u_y and u_θ with eccentricity are shown in Fig.7. The ratio R for the

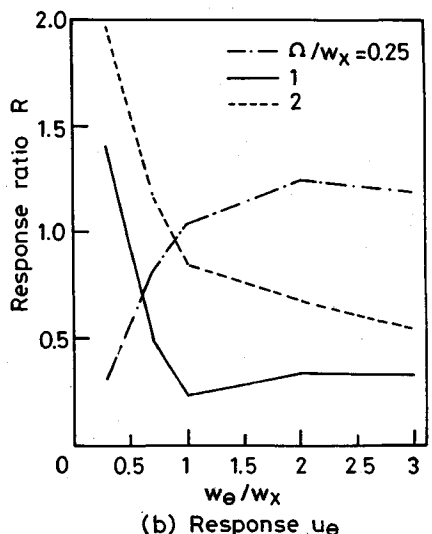
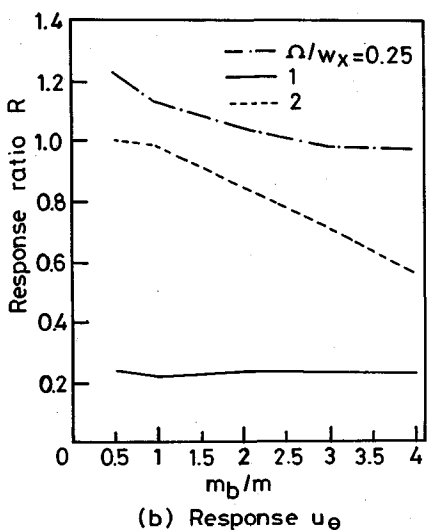
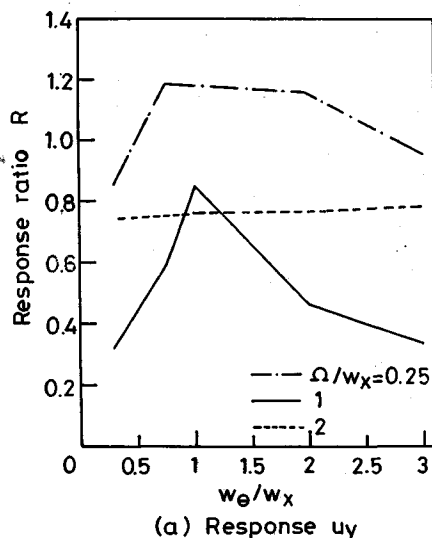
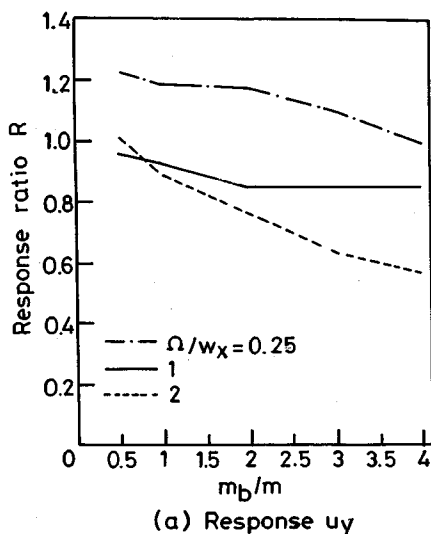


Fig.8 Variation of ratio R for u_y and u_θ against m_b/m .
 $T_x=1$ sec., $e_x/d=0.25$, $w_\theta/w_x=1$, $Q=50$ ton and $\alpha=0$.

Fig.9 Variation of ratio R for u_y and u_θ with w_θ/w_x .
 $T_x=1$ sec., $e_x/d=0.25$, $m_b/m=2$, $Q=50$ ton and $\alpha=0$.

response u_y increases with the increase in e_x/d . Same observation holds good for torsional response, u_θ . Thus, the effectiveness of base isolation is reduced for higher eccentricities. The influence of eccentricity on R depends upon the frequency of excitation. Note that the value of R for zero eccentricity shows the effectiveness of base isolation if the model shown in Fig.1 were idealized as 2-D system independently in the two directions (x and y). The figure clearly indicates that the effectiveness of base isolation is overestimated if the effect of torsional coupling is ignored and the system is idealized as 2D-model.

Effect of mass ratio (m_b/m)

In Fig.8, the variations of R for responses u_y and u_θ are plotted against mass ratio, m_b/m . It is observed that as the base mass increases, response of the system decreases for all values of Ω/w_x ratio. For higher frequency of excitation i.e. $\Omega/w_x=2$, the effect of mass ratio is more pronounced. Thus, the effectiveness of base isolation increases as the base mass of the system increases.

Effect of w_θ/w_x ratio

In Fig.9, the variations of R against w_θ/w_x are shown. w_θ is varied by changing the torsional mass of the deck without affecting the layout of the

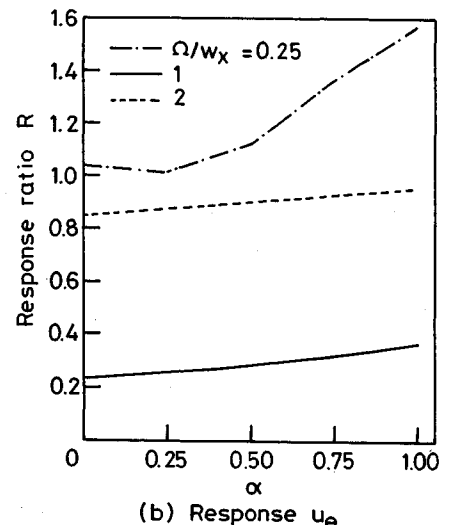
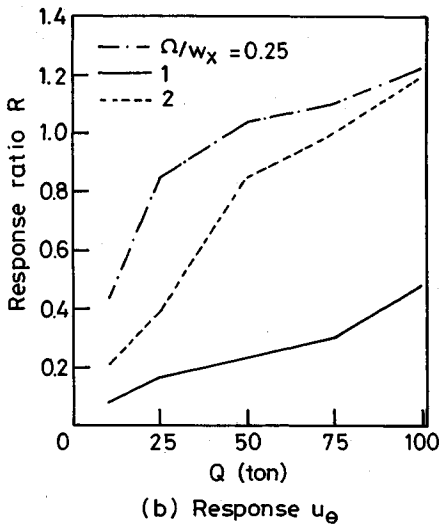
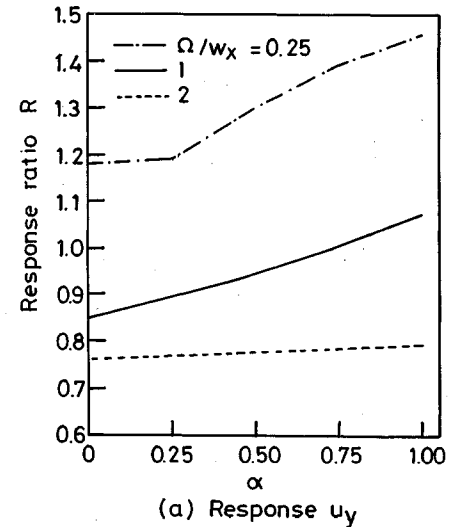
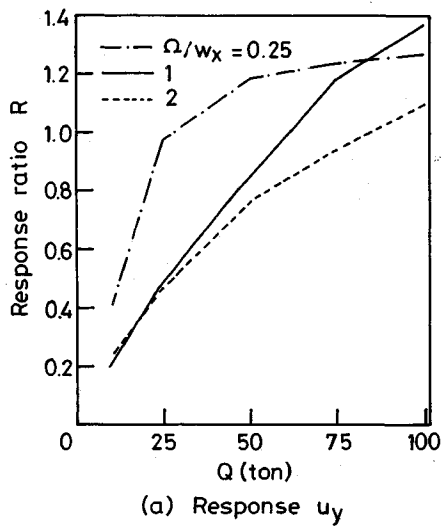


Fig.10 Variation of ratio R for u_y and u_θ against Q . $T_x=1$ sec., $e_x/d=0.25$, $m_b/m=2$, $w_\theta/w_x=1$ and $\alpha=0$.

Fig.11 Variation of ratio R for u_y and u_θ against α . $T_x=1$ sec., $e_x/d=0.25$, $m_b/m=2$, $Q=50$ ton and $w_\theta/w_x=1$.

isolators as described before. For the excitation frequencies $\Omega = 0.25 w_x$, the ratio R for the response u_y increases with the increase in w_θ/w_x in the range of $0 < w_\theta/w_x \leq 1$ showing less effectiveness of base isolation with the increase in w_θ/w_x . However, for $w_\theta/w_x > 1$, opposite effect is observed. For $\Omega = 2w_x$, the ratio R for the response u_y is insensitive to the variation of w_θ/w_x . For the excitation frequency $\Omega = w_x$ and $2w_x$, the ratio R for the response u_θ decreases significantly with the increase in w_θ/w_x in the range of $0 < w_\theta/w_x \leq 1$ showing effectiveness of base isolation for reducing torsional response. For $w_\theta/w_x > 1$, the ratio R

further decrease for $\Omega = 2w_x$, whereas for $\Omega = w_x$ it increase moderately. Thus, w_θ/w_x influences the effectiveness of base isolation in a complex manner. The base isolation for torsionally coupled system may become effective only for a limited range of the values of w_θ/w_x and excitation frequencies.

Effect of yield strength parameter, Q

In Fig.10, R is plotted for responses u_y and u_θ against the parameter, Q of the bearing. The ratio R increases with the increases in Q showing less effectiveness of base isolation. It is due to the fact that for low values of the yield strength parameter,

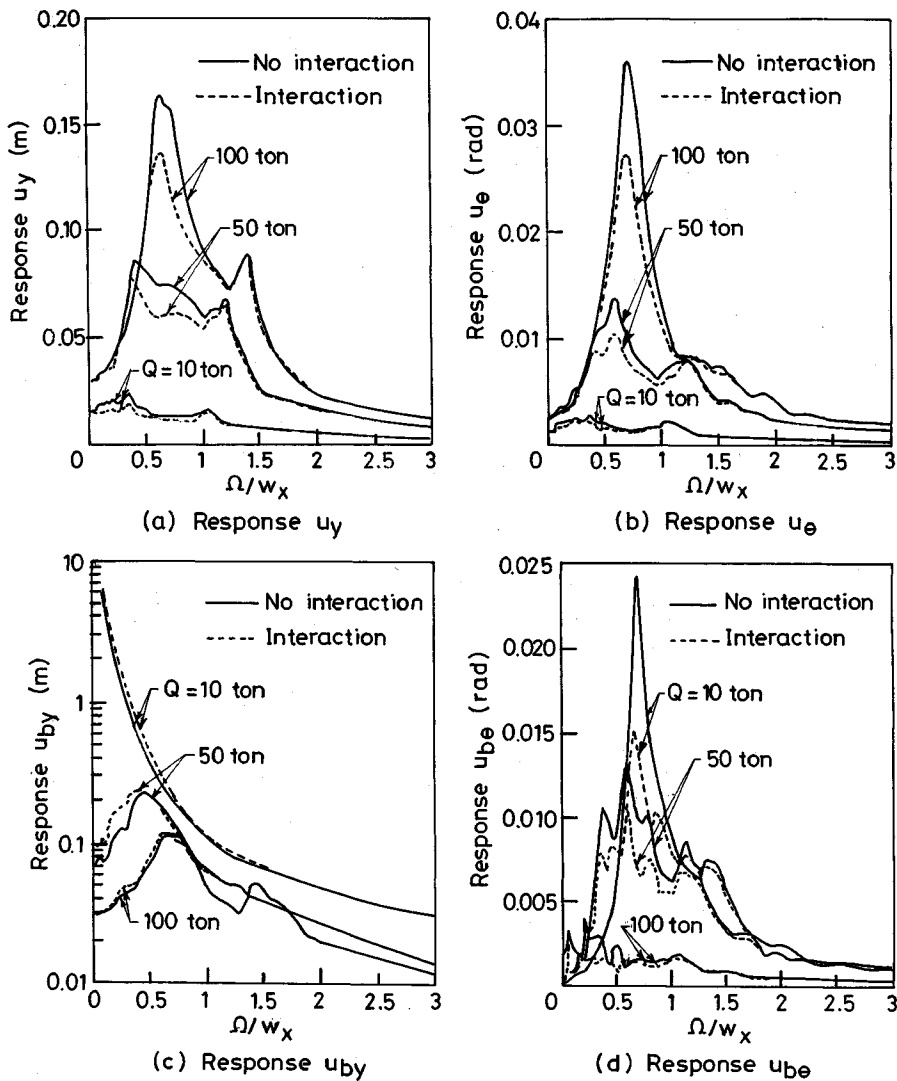


Fig.12 Difference between responses with and without interaction between restoring force. $T_x=1$ sec., $e_x/d=0.25$, $m_b/m=2$, $\alpha=0$ and $w_\theta/w_x=1$.

system undergoes more cycles of hysteresis loop leading to more energy dissipation. As a result, the response of the system is decreased and the value of R is reduced.

Effect of Stiffness Parameter, α

In Fig.11, the variation of R is plotted against the parameter α . It is observed that the effectiveness of base isolation decreases as α increases. The effectiveness is maximum at $\alpha=0$ (which is the case of elasto plastic bearing).

Effect of Restoring Force Interaction

In Fig.12, responses u_y , u_θ and u_{by} and $u_{b\theta}$ are plotted against excitation frequency for the yield strength parameter $Q=10, 50$ and 100 ton for two

cases (i) when the interaction between the restoring forces in the two directions (x and y) is considered on the force deformation relationship and (ii) when this interaction is ignored. For no interaction case, the off diagonal terms (which couples the restoring force in the two directions) of matrix $[G]$ in Equation (7) are taken as zero resulting in a uniaxial model of the bearing in the two directions. The responses u_y , u_θ and $u_{b\theta}$ are more for the case when interaction effect is not considered in the analysis. Thus, if the interaction effect is ignored, the effectiveness of base isolation is underestimated. Note that the base displacement u_{by} is less for no interaction case. Further, the

effect of interaction is more pronounced for the frequencies where maximum responses occurs.

CONCLUSIONS

The nonlinear response of a torsionally coupled base isolated system to harmonic base excitation is obtained and its behaviour is investigated for a set of important parametric variations. In particular, the influence of harmonic excitation frequency on the effectiveness of base isolation is examined. The effectiveness of base isolation is studied by comparing the responses of base isolated system with those of the fixed base system. The results of the study lead to the following conclusions :

- (1) For low values of uncoupled time period of fixed base system, the isolation is effective for the range of frequency greater than 0.5 times the uncoupled fixed base frequency. The effectiveness of base isolation becomes maximum under resonating condition.
- (2) The effectiveness of base isolation increases with the increase in base mass.
- (3) Effectiveness of base isolation decreases with the increase in the eccentricity of the system.
- (4) Effectiveness of base isolation in reducing torsional response significantly, increases with the increases in w_0/w_x (in the range $0 \leq w_0/w_x \leq 1$) for excitation frequency $\Omega > 0.5w_x$.
- (5) The effectiveness of base isolation decreases with the increase in yield strength of the bearing.
- (6) Post to pre-yielding stiffness ratio of the bearing signifying the hysteretic behaviour of the base isolation system considerably influences the effectiveness of base isolation for low values of the excitation frequency.
- (7) The restoring force interaction between two principal directions influences the response of torsionally coupled base isolated system and is significant near resonating condition.

REFERENCES

- 1) Constantinou, M. C. and Tadjbakhsh, I. G. : Probabilistic Optimum Base Isolation of Structures, Journal of Structural Engineering, ASCE, 109, 305~310, 1983.
- 2) Constantinou, M. C. and Tadjbakhsh, I. G. : The Optimum Design of a Base Isolation system with Friction Element, Earthquake Eng. and Struct. Dyn., 12, 203~214, 1984.
- 3) Kelly, J. M. and Beucke, K. E. : A Frictional Damped Base Isolation System with Fail-safe Characteristic, Earthquake Eng. and Struct. Dyn., 11, 33~56, 1983.
- 4) Keightley, W. O. : Building Damping by Coulomb Friction, Sixth World Conference on Earthquake Engineering, New Delhi, India, 1977.
- 5) Kelly, J. M. : A seismic base isolation : A Review and Bibliography, Soil Dynamics and Earthquake Engineering, 5, 202~216, 1986.
- 6) Kelly, J. M. and Hodder, S. B. : Experimental Study of Lead and Elastomeric Dampers for Base Isolation System in Laminated Neoprene Bearings, Bulletin of the New Zealand National Society for Earthquake Engineering, 15, 53~67, 1982.
- 7) Lee, D. M. and Medland, I. C. : Base Isolation Systems for Earthquake Protection of Multi Storey Shear Structure, Earthquake Eng. and Struct. Dyn., 7, 555~569, 1979.
- 8) Nagarajaiah, S., Reinhorn, A. M. and Constantinou, M. C. : Nonlinear dynamic analysis 3-D-base isolated structures, Journal of Struct. Eng., ASCE, 117, 2035~2054, 1991.
- 9) Mario Paz : Structural Dynamics-Theory and Computation, CBS Publishers and distributors, Delhi, 1987.
- 10) Park, Y. J., Wen, Y. K. and Ang, A. H. S. : Random vibration of hysteretic systems under bi-directional ground motion, Earthquake Eng. and Struct. Dyn., 14 (4), 543~557, 1986.
- 11) Pan, T. C and Kelly, J. M. : Seismic response of torsionally coupled Base Isolated Building, Earthquake Eng. and Struct. Dyn., 11, 749~770, 1983.
- 12) Skinner, R.I., Tyler, R. G., Heine, A. J. and Robinton, W. H. : Hysteretic Dampers for the Protection of Structure from Earthquake, Bulletin of the New Zealand National Society for Earthquake Engineering, 13, 22~36, 1980.
- 13) Wakabayashi, M., Fujiwara, T., Nakamura, T. and Bastov, T. : Experimental Study on the Dynamic Characteristic of Isolated Structures, Bull. Disaster Prevention, Inst. Kyoto Univ, 31, 151~169, 1981.
- 14) Wen, Y. K. : Method of Random Vibration of Hysteretic Systems, Journal of Engineering Mechanics Division, ASCE, 102, 249~263, 1976.

(Received May 21, 1992)